NASA TN D-1500

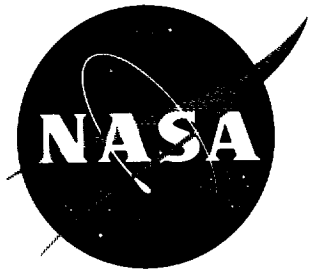

TECHNICAL NOTE

D-1500

A FREE-FLIGHT INVESTIGATION OF ABLATION OF A BLUNT BODY TO A MACH NUMBER OF 13.1

By Clyde W. Winters, William G. Witte, Bernard Rashis, and Russell N. Hopko

Langley Research Center
Langley Station, Hampton, Va.

NATIONAL AERONAUTICS AND SPACE ADMINISTRATION

WASHINGTON December 1962

NATIONAL AERONAUTICS AND SPACE ADMINISTRATION

TECHNICAL NOTE D-1500

A FREE-FLIGHT INVESTIGATION OF ABLATION OF A BLUNT BODY TO A MACH NUMBER OF 13.1

By Clyde W. Winters, William G. Witte, Bernard Rashis, and Russell N. Hopko

SUMMARY

A five-stage rocket-propelled research-vehicle system was flown to a maximum Mach number of 13.1 at an altitude of approximately 78,000 feet to determine ablation characteristics of Teflon in free flight. Continuous in-flight measurements were made using sensors developed by the National Aeronautics and Space Administration. The sensors were located on the blunted face of a nose cone constructed from Teflon, with one at the stagnation point and two others at a surface distance of 0.62 radius on opposite sides of the stagnation point. The ablated-length measurements were in close agreement with analytical predictions. The analytical predictions, upon inclusion of the pertinent material property values, should be applicable to other materials as well as Teflon.

INTRODUCTION

Considerable research work on ablating materials has been conducted in ground facilities such as ceramic-heated and arc-heated air jets. In general, the early work in this field had as a prime objective the qualitative assessment of the potential of ablating materials; for example, see references 1 and 2.

As work progressed in this field, it became apparent that the heat-blocking capacity or potential of ablating materials depended very strongly on the enthalpy potential across the boundary layer. In reference 3, experiments were conducted at both low and high enthalpy potentials (100 Btu/lb to 7,000 Btu/lb) and the results clearly indicated the substantial effect of this parameter. As the experimental work progressed, analytical procedures were developed to predict effective heats of ablation (refs. 4 and 5).

Once these ablation parameters were clearly defined, ablating materials were quickly accepted as a very effective means of providing heat protection. In view of NASA objectives to fly spacecraft to the moon and beyond with subsequent reentry in the earth's atmosphere, the Langley Research Center initiated a flight-test research project that would provide confirmation of the analytical methods of predicting ablation rates. The data would thus provide a basis for the design information needed for the proposed missions with high velocity requirements.

Prerequisite to the accomplishment of this task was the development of a technique that would enable measurement of the pertinent ablation data during free flight. As a result of this effort, an ablation sensor was developed that was capable of providing continuous in-flight measurements. The details of this sensor and its development are given in reference 6.

Although other materials were investigated, the ablation sensor developed worked only for Teflon. The reasons are that Teflon had compatible dielectric properties and ablates directly to a gas, these conditions being requirements for this particular sensor design. Thus, for this flight test, Teflon was used as the ablating material.

This paper presents the results obtained from a free-flight investigation of a five-stage vehicle with an ablating Teflon nose cone fixed to the fifth stage. At third-stage ignition, the vehicle had a reentry angle of -8°. This occurred at an altitude of 85,000 feet and a velocity of 980 feet per second. The ablation measurements were obtained at Mach numbers from 9.0 to 13.1 and at free-stream Reynolds numbers per foot from 0.5×10^6 to 5.4×10^6.

SYMBOLS

C_p	specific heat, Btu/lb-$^{\circ}$F
H	enthalpy, Btu/lb
h	altitude, ft
h_{eff}	effective heat of ablation, Btu/lb
h_i	heat-transfer-coefficient enthalpy, Btu/(sq ft)(sec)($^{\circ}$R)
l	ablated length, in.
M	Mach number
$\dot{m}$	ablation rate, lb/(sq ft)(sec)
q	heating rate, Btu/(sq ft)(sec)
R	Reynolds number per foot
r	radius of nose, ft
r_c	radius of curvature of nose, 0.5 ft
s	distance along surface, measured from stagnation point, in.
T	temperature, $^{\circ}$R

t time, sec

V velocity, ft/sec

x range, ft

ρ density, slugs/cu ft

Subscripts:

aw adiabatic wall

c coolant

l local

o initial condition

sl sea level

t stagnation point

w wall

∞ free stream

TEST MODEL

The model, details of which are given in figure 1, was a body of revolution 5.20 inches in length, having a blunted face with r/r_c of 1/3 and an afterbody with a 10^o flare. The model was machined from a single piece of Teflon. A magnesium liner inserted in the Teflon shell provided the means of attachment to the launch-vehicle system.

The ablation sensors were mounted so that their longitudinal axes were normal to the surface. One sensor (sensor 2) was located at the stagnation point and two others (sensors 1 and 3) were located at $s/r = 0.62$. A fourth (sensor 4) was located on the flare 1.12 inches from the flare-cylinder junction. A photograph of the model and fifth stage is shown as figure 2.

LAUNCH VEHICLE

The launch-vehicle system consisted of five stages with an Honest John M6 rocket motor as the first stage. The second and third stages were Nike M5 motors. The fourth stage was an XM19 Recruit motor, and the fifth-stage sustainer was a T55 rocket motor. Complete details as to the launch vehicle and its capabilities are given in reference 7. Figure 3 shows the vehicle system just prior to launch.

INSTRUMENTATION

A standard NASA eight-channel telemeter for use with a five-stage vehicle, located behind the nose and in front of the fifth-stage motor (see fig. 2), was used in telemetering the data from the model. Four of the channels were used for linear accelerometers: two longitudinal (thrust and drag), one normal, and one transverse. Three of the channels were utilized for the ablation sensors mounted in the blunted face. The remaining channel was used for an ablation sensor mounted in the 10° flared afterbody. This sensor became defective prior to the time that pertinent data were obtained. Analysis of the malfunction indicated that one or both of the leads attached to the sensor became loose or broken.

Details of the sensor are shown in figure 4. The condenser plates are cut from a sheet of aluminum-coated Teflon, with the aluminum coating on only one surface. The coating is approximately 0.00005 inch in thickness and the total thickness of the Teflon and plating is approximately 0.001 inch. The condenser plates are cut as shown with the two strips forming the leads. The small strip of coating removed at the center provides the insulating region between the two plate areas. The plates are wrapped around the condenser rod exactly twice and the unit (rod and plates) is then press fitted into the sensor body. Thin strips of silver foil are then cemented to the plate leads. It was at these cemented joints that an opening or break probably occurred for the malfunctioning sensor. Complete details of the sensors are given in reference 6.

FLIGHT TRAJECTORY

The prelaunch computed trajectory assumed an elevation angle of 72° and an azimuth angle of 90° (measured clockwise from true north). This trajectory is standard for the launch vehicle used in this test. The measured flight trajectory, altitude plotted against range, is shown in figure 5. The data points were obtained using an NASA modified SCR-584 radar.

Time histories of the velocity and altitude are shown in figure 6(a). The curves shown were obtained from the radar data. As a check on the radar data, the histories of the longitudinal accelerometers were integrated. The values obtained, as shown by the circular symbols, essentially duplicate the velocity-time curve obtained from the radar.

Figure 6(b) shows the time histories of Mach number and free-stream Reynolds numbers per foot. Figure 6(c) shows the ambient values of density and temperature plotted against time. The variations of density, temperature, and wind with altitude were measured to an altitude of 75,000 feet by using a radiosonde which was tracked by a Rawin set AN/GMD-1A. Standard atmospheric conditions (ref. 8) agreed fairly well with the measured radiosonde data for altitudes up to 44,000 feet. However, for the altitude range 44,000 feet to 75,000 feet, the standard conditions coincided with the radiosonde data. It was thus assumed that the standard data would apply closely up to peak altitude (85,000 feet) and these data were used for altitudes above 75,000 feet.

DATA REDUCTION

The ablation sensors used do not indicate length changes directly. The results as received by telemetry are in the form of sensor frequency against flight time. In order to obtain length changes as a function of time, a calibration curve of frequency changes as a function of length change must be previously determined. The method consists of measuring the change in sensor capacitance due to the removal of sensor material. The capacitance change is then related to the frequency by the procedure described in reference 6. Since the removal of sensor material negates use of the sensor for flight, identically constructed sensors were used to obtain the calibration curves for the flight units. A typical calibration curve is shown in figure 2 of reference 6.

The effective heat of ablation h_{eff} is defined as the net heat input evaluated at the temperature of the ablating surface divided by the rate of ablation, or

$$h_{eff} = \frac{q}{\dot{m}}$$

where the ablation rate $\dot{m}$ is the product of the Teflon density and the time rate of length change or dl/dt.

The stagnation-point heat inputs q_t (surface radiation negligible) were computed from the following empirical formula from reference 9 (in the notation of the present paper):

$$q_t = \frac{17{,}600}{\sqrt{r}} \sqrt{\frac{\rho_\infty}{\rho_{sl}}} \left(\frac{V_\infty}{26{,}000} \right)^{3.15} \left[\frac{H_{aw} - H_w}{H_{aw} - (H_w)_{300^\circ K}} \right]$$

The heating rates as calculated from the above relationship of reference 9 were corrected for the effects of bluntness according to figure 3 of reference 10.

The values of the temperature of the Teflon ablating surface T_w were computed by using the analytical procedure described in reference 11. Briefly, in this method the Teflon ablating surface is assumed to be analogous to a burning surface and the surface temperature to be essentially the burning temperature and thus dependent only on the burning rate, or what would be the ablation rate in the case of ablating materials, and the material properties such as density, thermal conductivity, and specific heat. Since the ablation rates are known from the sensor measurements the values of T_w were read directly from the curve for Teflon given in figure 4 of reference 11.

The specific heat $c_{p,c}$ refers to the Teflon vapor. It was assumed that Teflon sublimes to a vapor state consisting mainly of C_2F_4 molecules, having a molecular weight of approximately 100. A curve of c_p plotted against temperature for this vapor state is given in figure 10 of reference 5.

The heat-transfer coefficients for the sensors at $s/r = 0.62$ were obtained from figure 7 which shows the heat-transfer-coefficient variation with s/r position for a nominal Mach number of 3.51. The data of figure 7 were obtained from tests conducted in Langley Unitary Plan wind tunnel with an Inconel calorimeter configuration that was identical in shape and size with the flight model. Previous experimental and analytical work (ref. 10) have verified that the heat-transfer distribution across a surface behind a strong bow shock remains essentially constant over a wide range of free-stream Mach numbers. Basically, this is because the surface pressure distribution is virtually unaffected by free-stream Mach number.

Figure 8 shows the heat inputs q that were calculated for the three sensor locations. No values are shown for times prior to 89 seconds, since the sensors indicated no measurable ablation. Also, no values are shown for times after 91 seconds, since at this time telemetry signals from the sensors were lost. However, accelerometer data were obtained to 94.5 seconds.

RESULTS AND DISCUSSION

Figure 9 shows the measured ablated-length ratios

$$\frac{\Delta l_{\frac{s}{r}=0.62}}{\Delta l_{\frac{s}{r}=0}}$$

as a function of the flight time. These ratios were obtained by normalizing the values measured for the sensors at $s/r = 0.62$ by dividing by the values measured for the stagnation-point sensor. The ablated-length ratios are by definition equal to the heat-transfer-coefficient ratio

$$\frac{h_{i,\frac{s}{r}=0.62}}{h_{i,\frac{s}{r}=0}}$$

As indicated in figure 9, the measured ablated-length ratios are consistent (within 6 percent) with the mean curve of heat-transfer coefficient obtained from Unitary Plan wind-tunnel results. In order to compare the measured flight ablated-length data with the analytical predictions of reference 5, the curve shown in figure 7 of reference 5 was used and is the basis for figure 10 of this report. This curve represents the theoretical relationship for the three-dimensional laminar stagnation-point ablation of Teflon. The analysis of reference 5, which applies only to quasi-steady-state ablation (penetration of heat into solid material is negligible as compared to the rate at which material ablates), relates the mass transfer effect to what is basically an enthalpy or velocity parameter, as indicated in the following expression:

$$\left(H_{aw} - H_{w,air}\right)\frac{c_{p,c}}{c_{p,l}}\left(\frac{T_l}{T_w}\right)^{0.19}$$

The solid-line portion of the curve of figure 10 represents the enthalpy-parameter range covered by this flight investigation.

With the variation of the above parameter known, the ablation rates may be determined by the following procedure. An ablation rate $\dot{m}$ is assumed. For this assumed $\dot{m}$, the values of T_w and $c_{p,c}$ are obtained from references 10 and 5, respectively, thus giving all the quantities needed for the computation of the enthalpy parameter and the heat input q.

The corresponding h_{eff} is read from figure 10, and $\dot{m}$ is computed from the relation

$$\dot{m} = \frac{q}{h_{eff}}$$

The procedure is repeated with the computed value of $\dot{m}$ to determine the new values of the enthalpy parameter and heat input and is continued until the value computed for $\dot{m}$ agrees with the value assumed at the start of the computation.

Once $\dot{m}$ as a function of time has been computed, the ablated length changes with time are obtained from the relationship

$$l - l_o = \frac{1}{\rho}\int_0^t \dot{m}\, dt$$

since

$$\frac{dl}{dt} = \frac{\dot{m}}{\rho}$$

The curves in figure 11 represent the predicted variation of ablated length with time as calculated by using the solid-line portion of the curve in figure 10. The symbols denote the actual measurements. Sensor 2 was located at the stagnation point of the blunted face. Sensors 1 and 3 were located at $s/r = 0.62$. The variation of length change with time is essentially the same for all three sensors. The total lengths ablated ranged from 0.0275 to 0.0287 inch. The agreement between the calculated curves and the measured data is quite good. With the exception of a few data points, the data agree well with the calculated variation.

The close agreement between the measurements and the predicted values of the ablated length indicates that the variation of the Teflon effective heat of ablation during the flight test would be that shown by the solid-line portion of the

curve of figure 10. It should be noted that the analysis of reference 5, upon inclusion of the pertinent material property values, applies to other materials as well as Teflon.

CONCLUDING REMARKS

A five-stage rocket-propelled research-vehicle system was flown to a maximum Mach number of 13.1 at an altitude of approximately 78,000 feet. Continuous in-flight measurements of ablated length were made using sensors developed by NASA. The sensors were located on the blunted face of a nose cone constructed from Teflon, with one at the stagnation point and two others at a surface distance of 0.62 radius on opposite sides of the stagnation point.

The ablated-length measurements were in close agreement with analytical predictions. Except for a few data points, agreement was consistent with the predicted variation. The analytical procedure, upon inclusion of the pertinent material property values, should also apply to other materials.

Langley Research Center,
National Aeronautics and Space Administration,
Langley Station, Hampton, Va., August 17, 1962.

REFERENCES

1. Rashis, Bernard, Witte, William G., and Hopko, Russell N.: Qualitative Measurements of the Effective Heats of Ablation of Several Materials in Supersonic Air Jets at Stagnation Temperatures up to 11,000° F. NACA RM L58E22, 1958.

2. Bond, Aleck C., Rashis, Bernard, and Levin, L. Ross: Experimental Ablation Cooling. NACA RM L58E15a, 1958.

3. Rashis, Bernard, and Walton, Thomas E., Jr.: An Experimental Investigation of Ablating Materials at Low and High Enthalpy Potentials. NASA TM X-263, 1960.

4. Roberts, Leonard: A Theoretical Study of Stagnation-Point Ablation. NASA TR R-9, 1959. (Supersedes NACA TN 4392.)

5. Rashis, Bernard, and Hopko, Russell N.: An Analytical Investigation of Ablation. NASA TM X-300, 1960.

6. Winters, Clyde W., and Bracalente, Emedio M.: A Sensor for Obtaining Ablation Rates. NASA TN D-800, 1961.

7. Swanson, Andrew G.: A Five-Stage Solid-Fuel Sounding-Rocket System. NASA MEMO 3-6-59L, 1959.

8. The Rocket Panel: Pressures, Densities, and Temperatures in the Upper Atmosphere. Phys. Rev., vol. 88, no. 5, Second ser., Dec. 1, 1952, pp. 1027-1032.

9. Detra, R. W., Kemp, N. H., and Riddell, F. R.: Addendum to 'Heat Transfer to Satellite Vehicles Re-entering the Atmosphere.' Jet Propulsion, vol. 27, no. 12, Dec. 1957, pp. 1256-1257.

10. Stoney, W. E., Jr.: Aerodynamic Heating of Blunt Nose Shapes at Mach Numbers up to 14. NACA RM L58E05a, 1958.

11. Steg, Leo: Materials for Re-Entry Heat Protection of Satellites. [Preprint] 836-59, American Rocket Soc., June 1959.

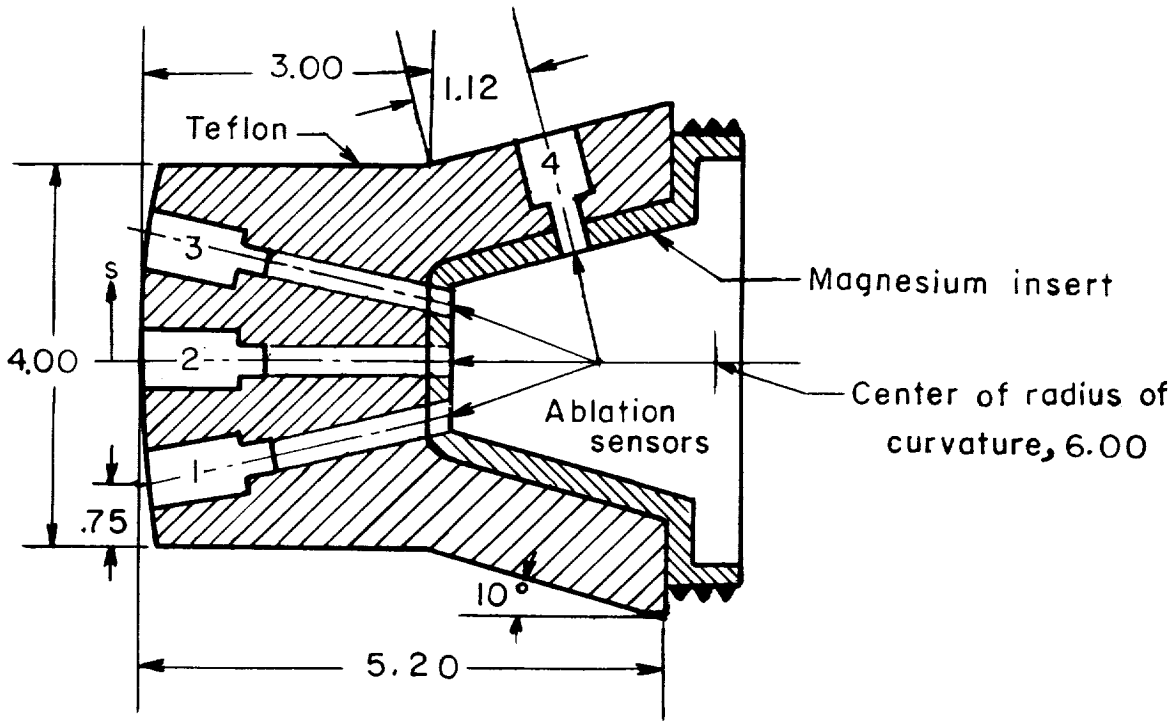

Figure 1.- Model details, dimensions, and location of ablation sensors. All dimensions are in inches.

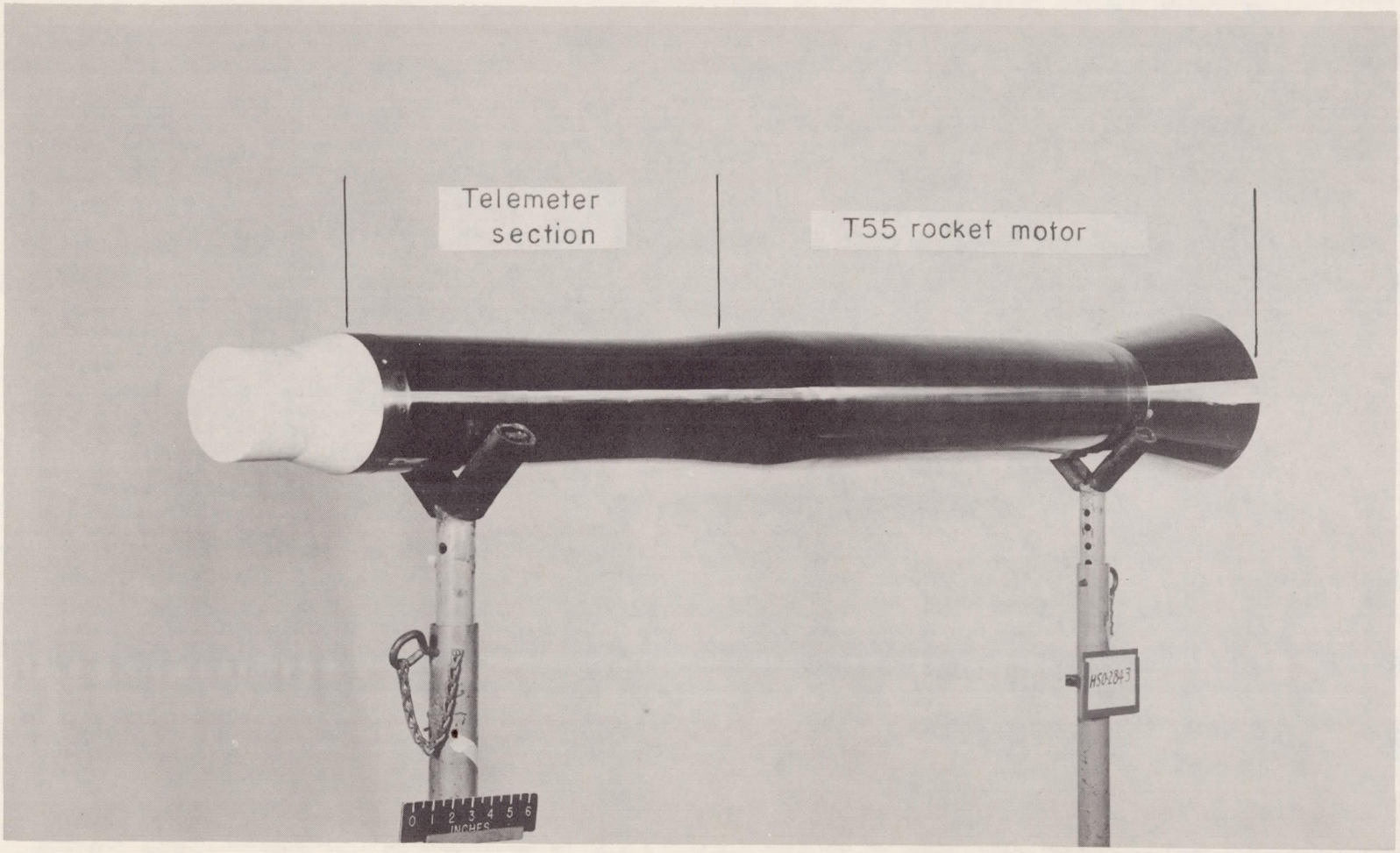

Figure 2.- Teflon model and fifth stage. L-60-7781.1

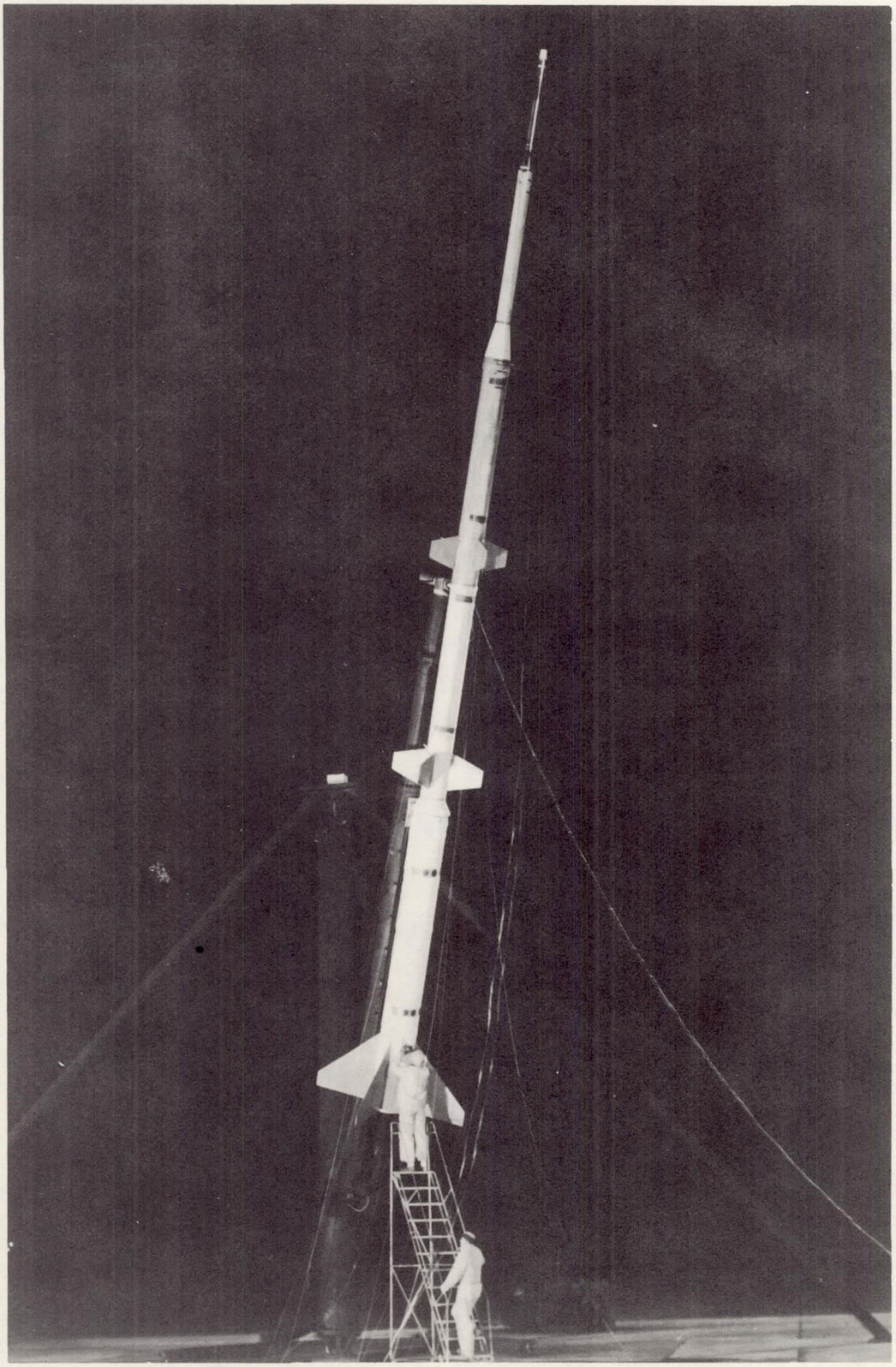

Figure 3.- Vehicle in launch position. L-60-8152

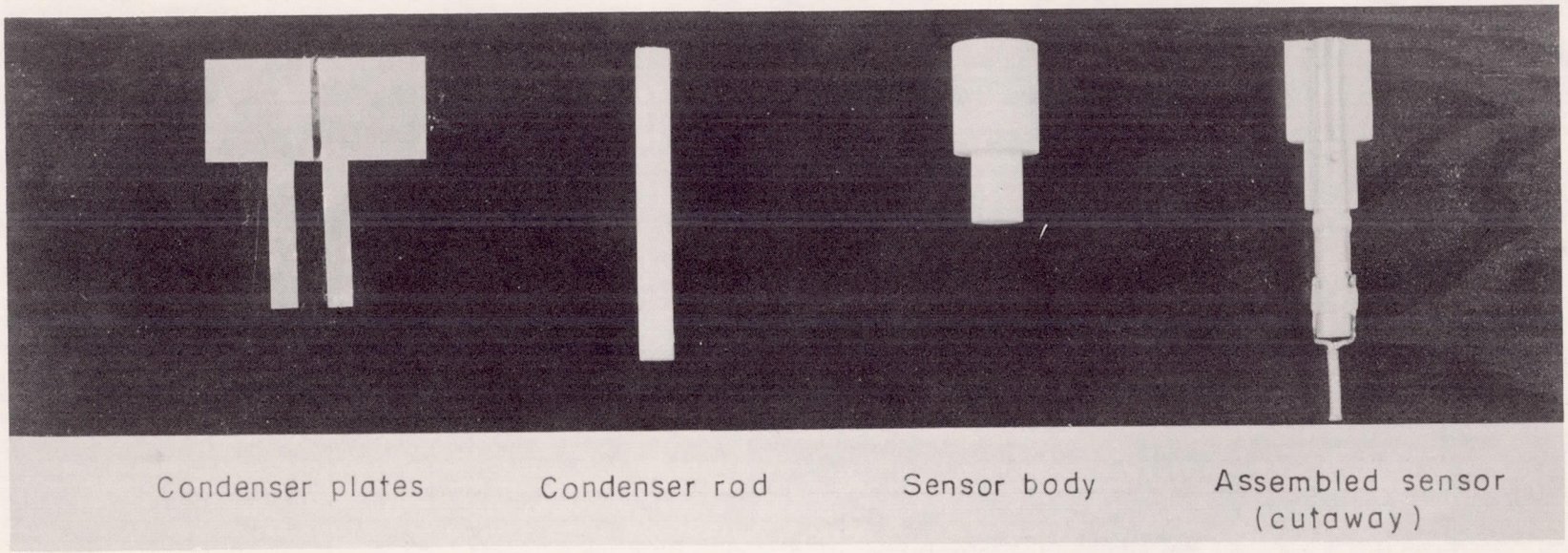

Figure 4.- Details of ablation sensor. L-61-51

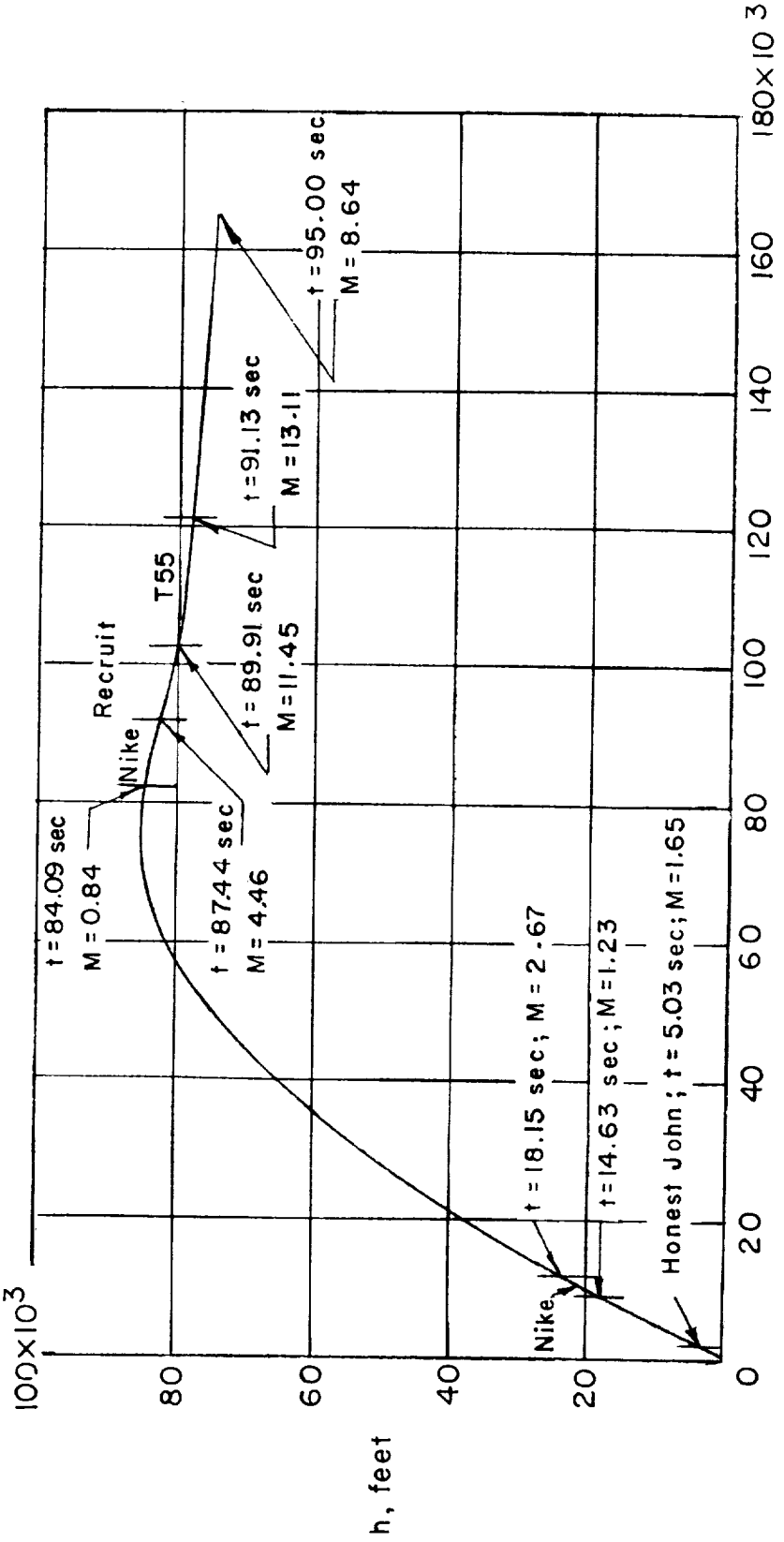

Figure 5.- Model trajectory.

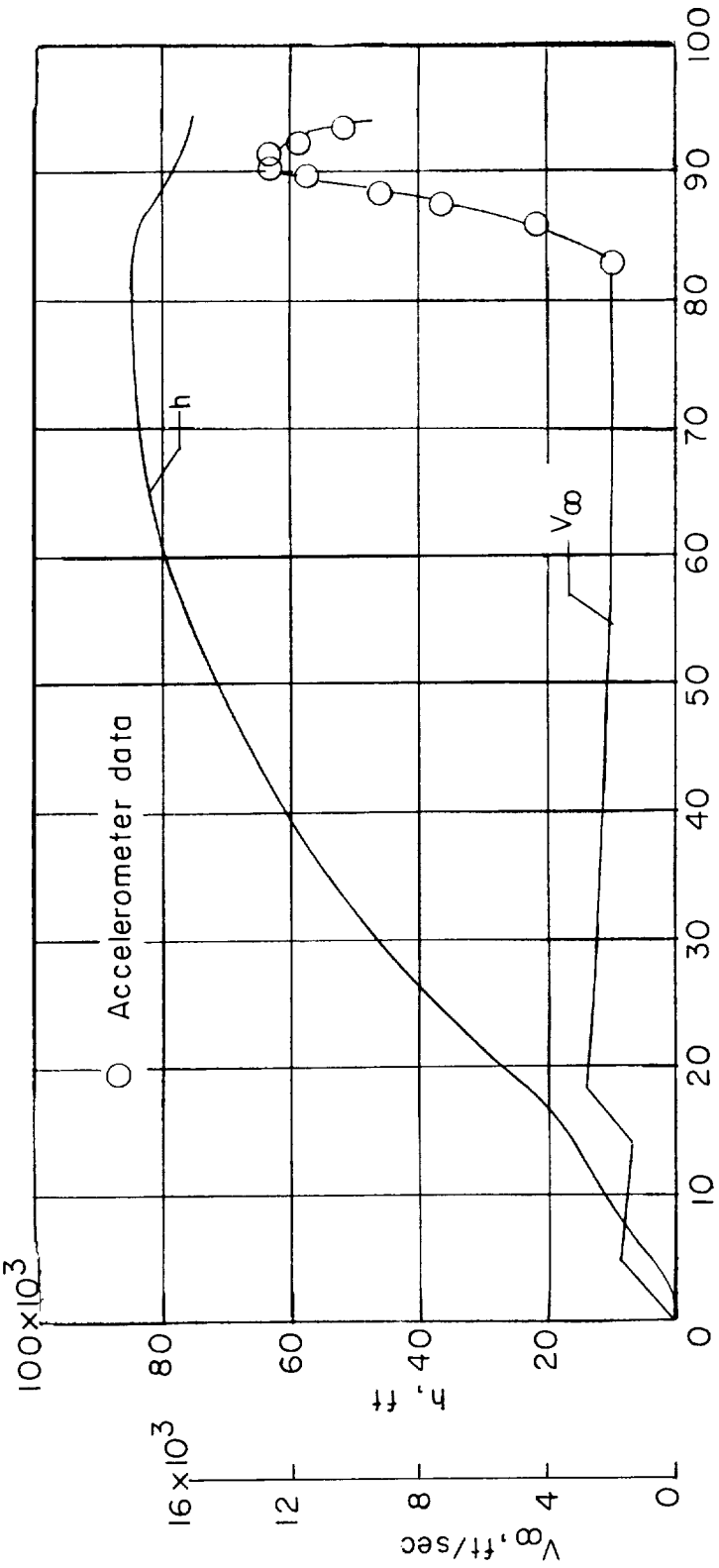

(a) Model velocity and altitude.

Figure 6.- Time histories of flight conditions.

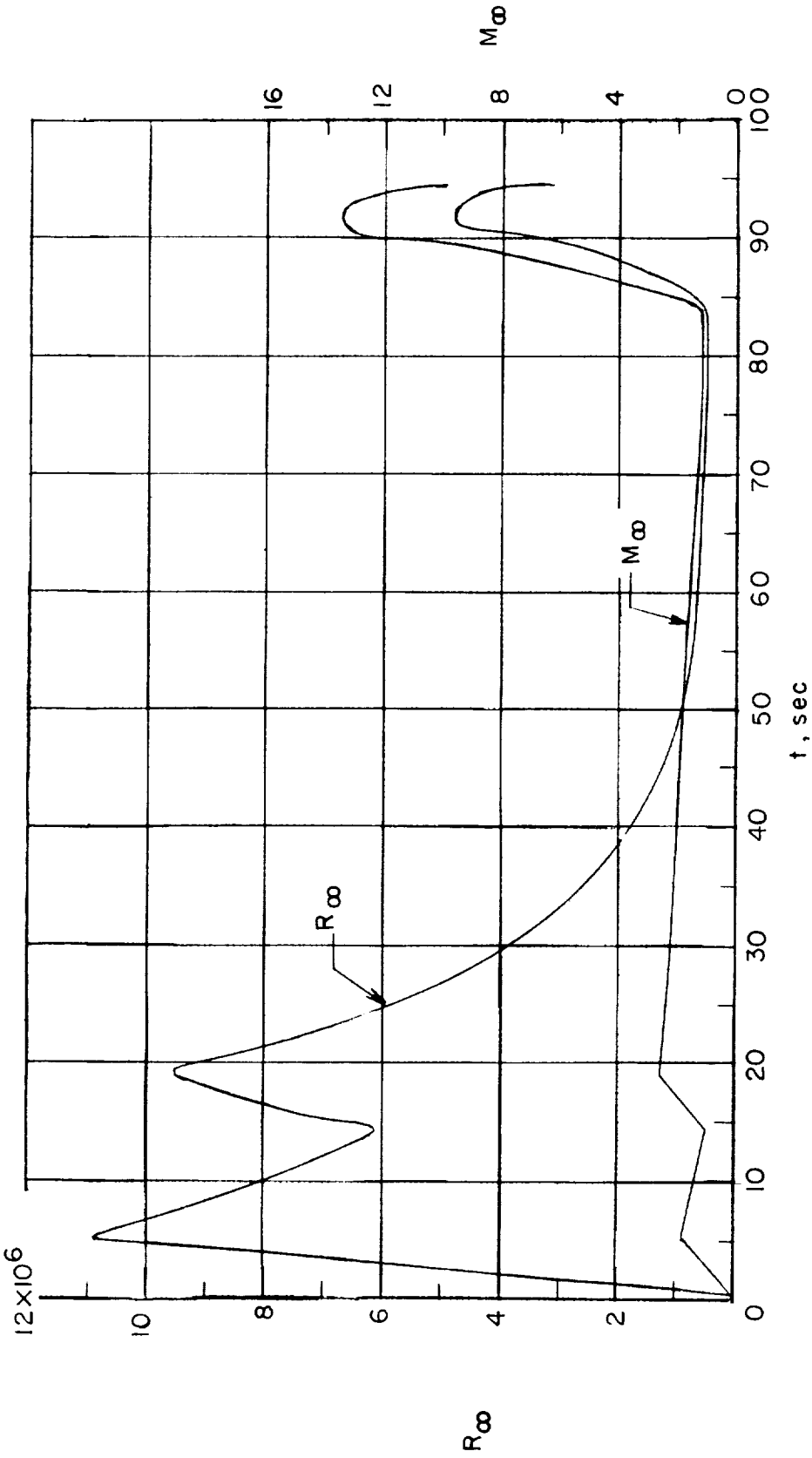

(b) Free-stream Mach number and free-stream Reynolds number per foot.

Figure 6.- Continued.

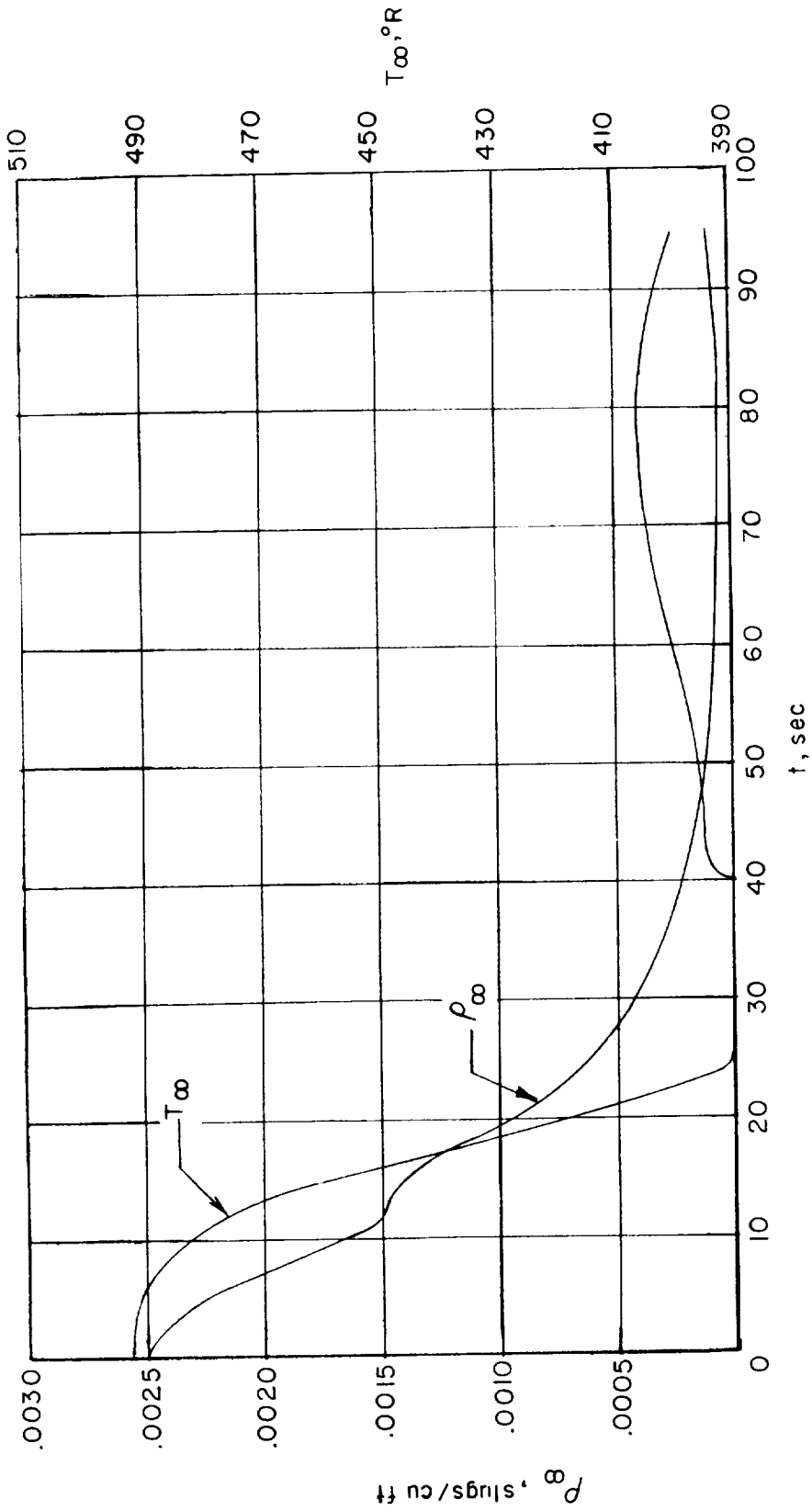

(c) Free-stream density and free-stream temperature.

Figure 6.- Concluded.

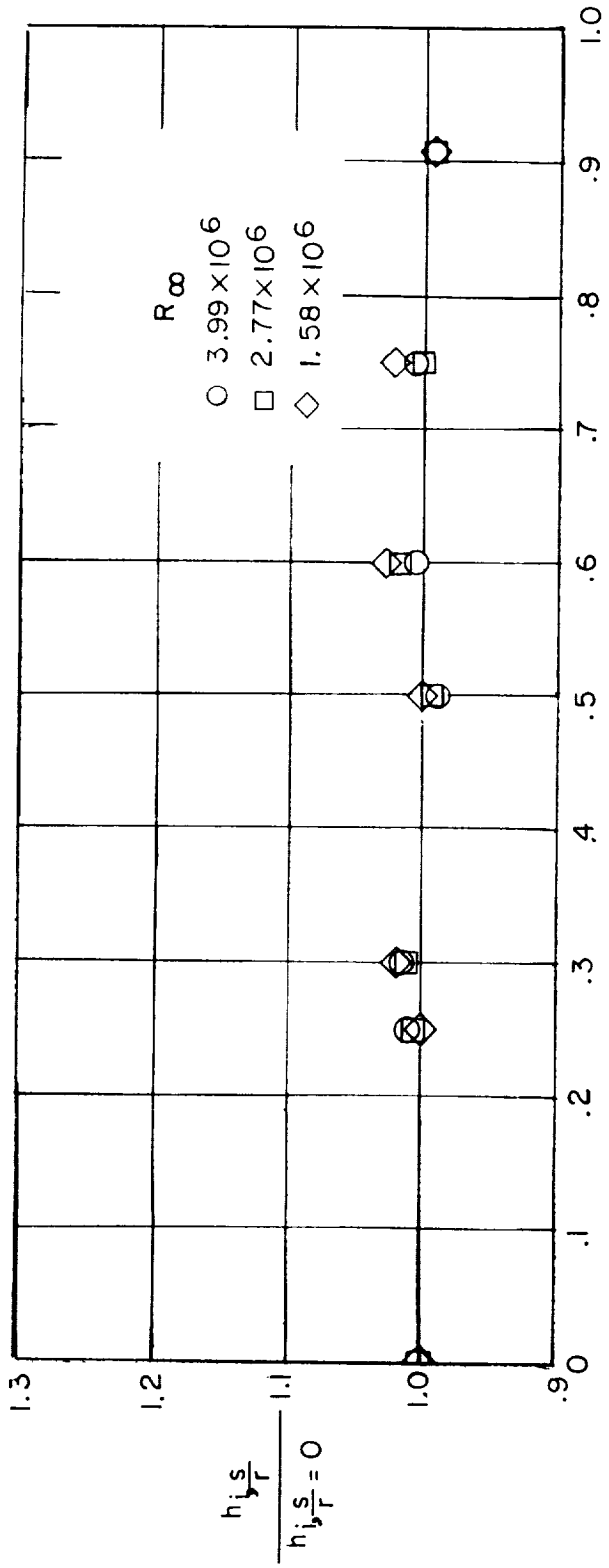

Figure 7.- Effects of Reynolds number on heat-transfer-coefficient distribution across face of Inconel calorimeter for tests made in Langley Unitary Plan wind tunnel. $M_\infty = 3.51$.

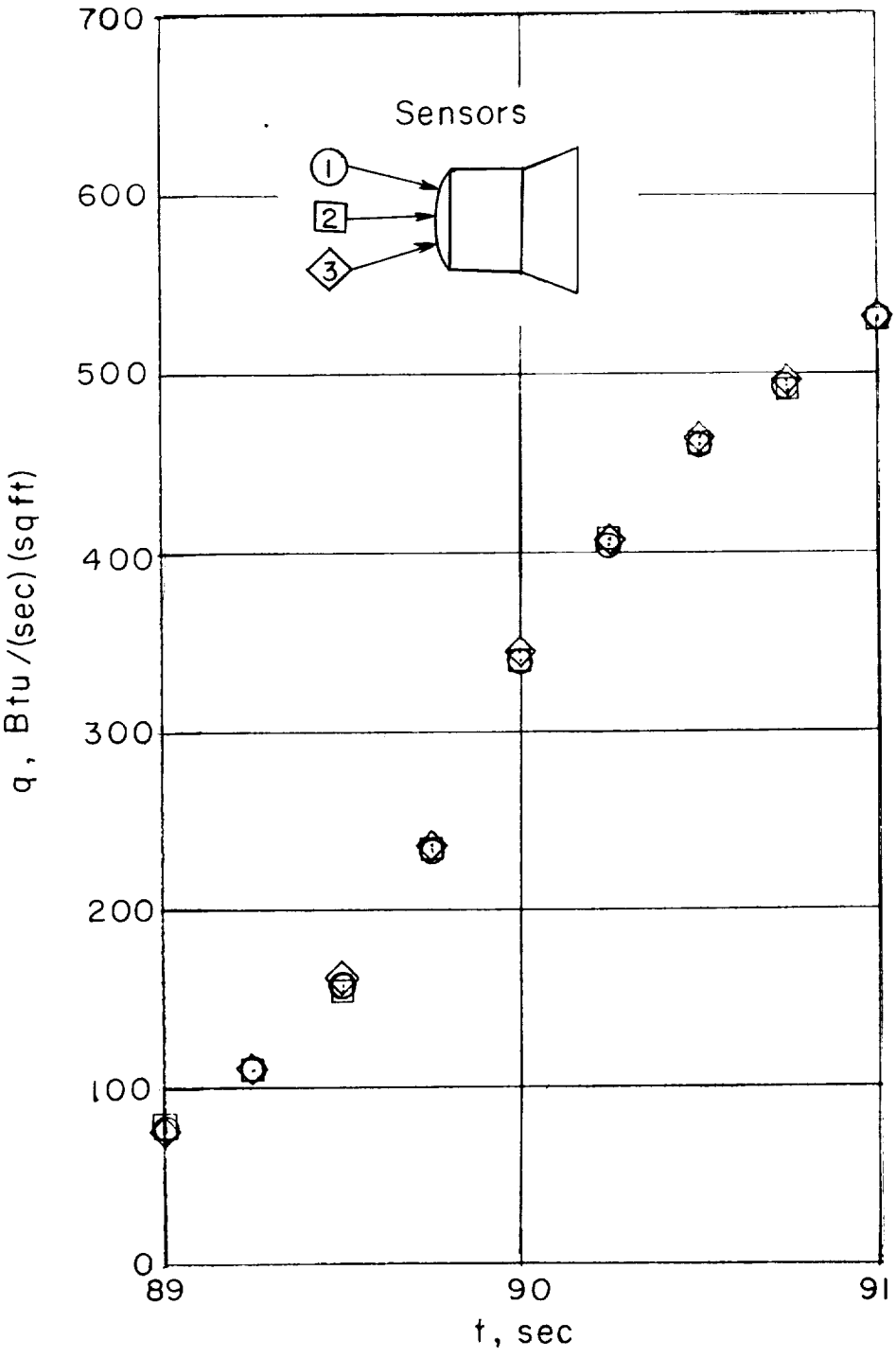

Figure 8.- Theoretical heating rates calculated for three sensor locations on front face.

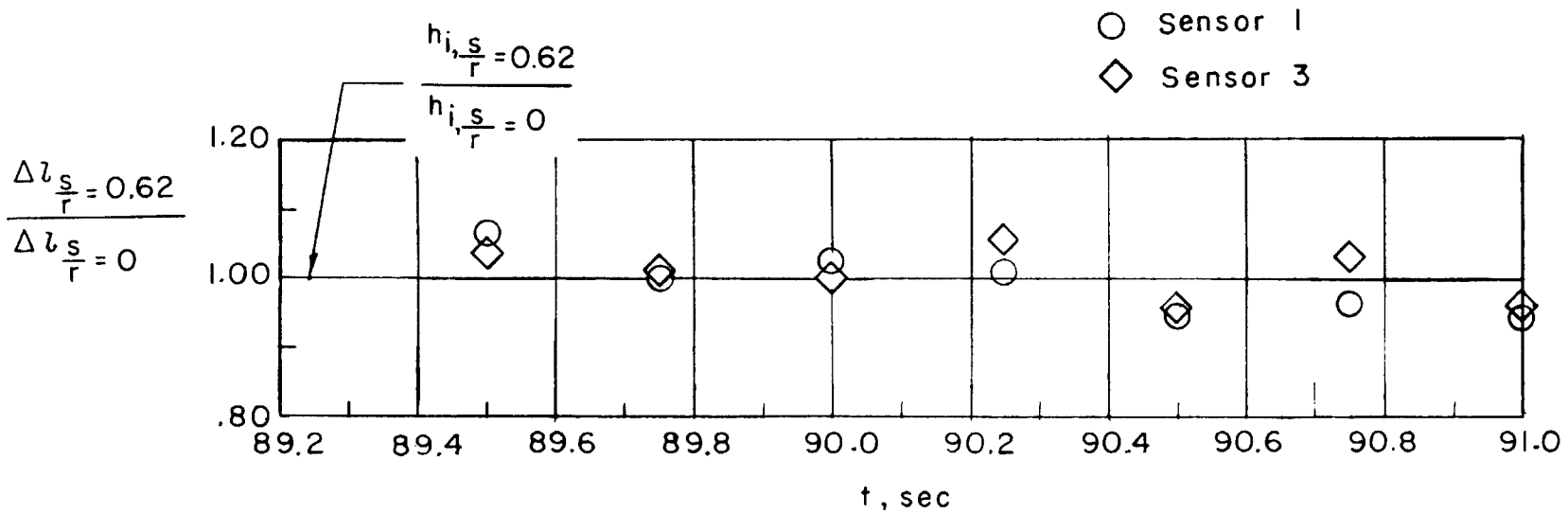

Figure 9.- Comparison of ablation distribution with heat-transfer-coefficient distribution for sensors at $\frac{s}{r} = 0.62$.

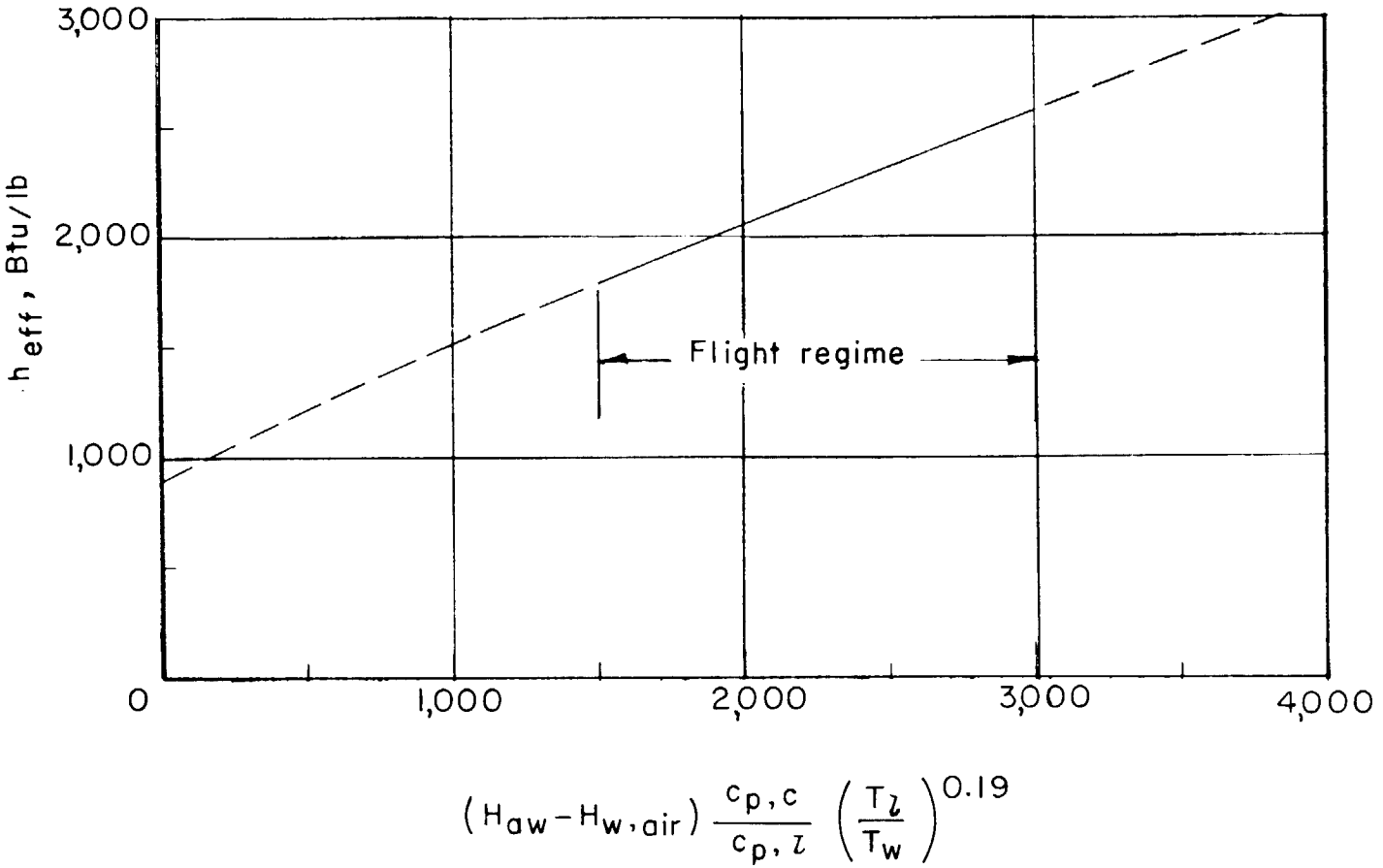

Figure 10.- Predicted effectiveness of Teflon material (based on data from ref. 5).

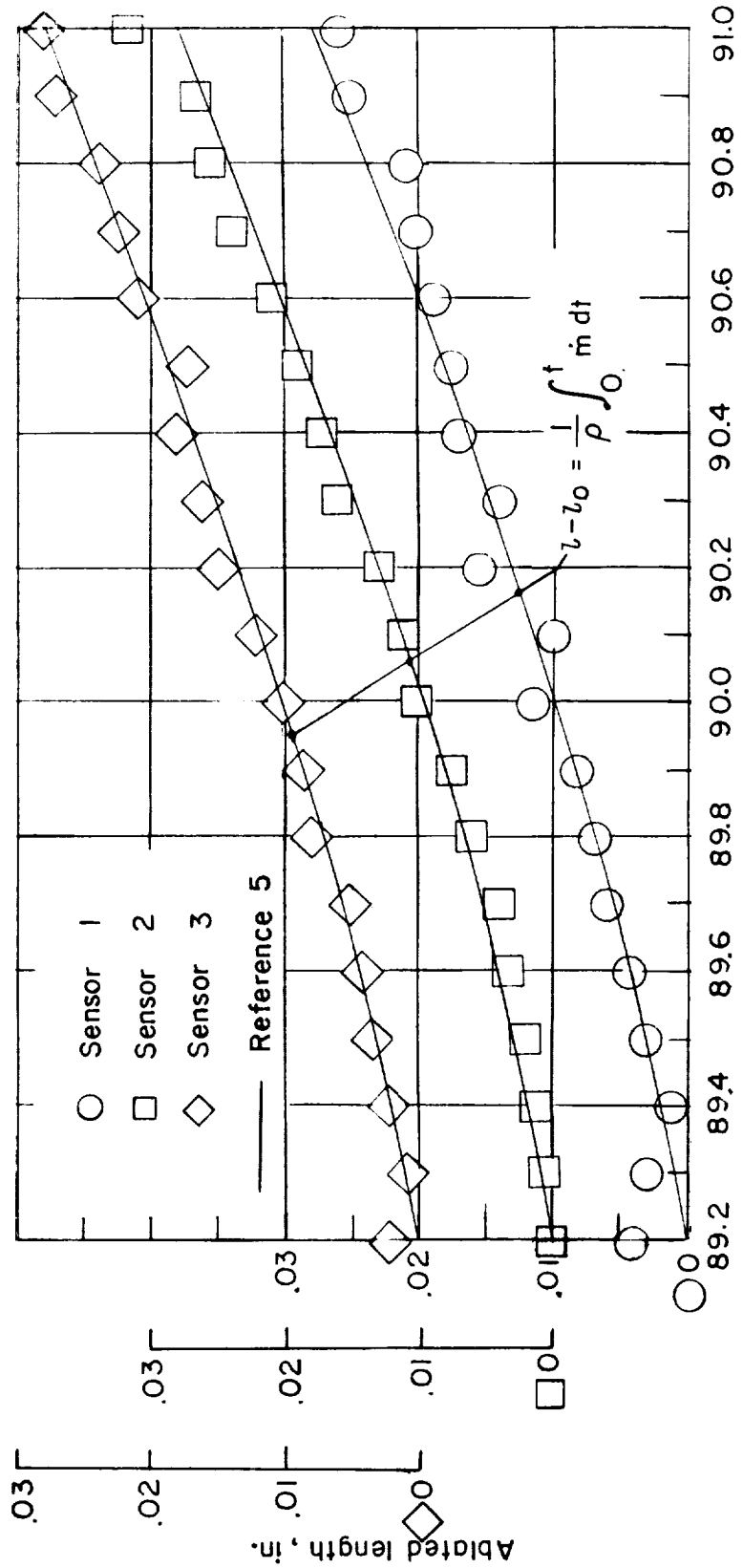

Figure 11.- Time histories of ablated lengths for ablation sensors 1, 2, and 3.

NASA-Langley, 1962 L-3062